Partitioning the genomic journey to becoming *Homo sapiens*

Luca Pagani[1,2], Riccardo Bertazzon[1], Vasili Pankratov[2,3], Leonardo Vallini[4], Davide Marnetto[5], Adeline Morez[1], Hélios Delbrassine[1], Francesca Carollo[1], Maurizio D'Esposito[6+], Ilaria Granata[6], En En Teo[7], Aswini Leela Loganathan[7], Pille Hallast[8], Charles Lee[8], Qasim Ayub[7], Massimo Mezzavilla[1]

Affiliations

1 Department of Biology, University of Padova, Via Ugo Bassi 58/B, 35131, Padova, Italy

2 Institute of Genomics, University of Tartu, Riia 23/b, 51010 Tartu, Estonia

3 Bioinformatics Research Centre, Aarhus University, Universitetsbyen 81, 3., Building 1872, DK-8000 Aarhus C Denmark

4 Institute of Organismic and Molecular Evolution, Palaeogenetics Group, Johannes Gutenberg University, Mainz 55128, Germany

5 Department of Neurosciences, University of Turin, 10126, Turin, Italy

6 Istituto di Calcolo e Reti ad alta prestazione, CNR, 80131, Naples, Italy

7 Monash University Malaysia Genomics Facility, School of Science, Monash University, 47500 Bandar Sunway, Selangor Darul Ehsan, Malaysia

8 The Jackson Laboratory for Genomic Medicine, Farmington, CT, USA

Corresponding authors: luca.pagani@unipd.it, massimo.mezzavilla@unipd.it

Abstract

What makes us human? *Homo sapiens* diverged from its ancestors in fundamental ways, as reflected in recent genomic acquisitions, such as the PAR2-Y chromosome translocation. Here we show that despite morphological and cultural differences between modern and archaic humans, these human groups share these recent acquisitions. Our modern lineage shows recent functional variants in only 56 genes, of which 24 are linked to brain functions and skull morphology. Nevertheless, these acquisitions failed to introgress into Neanderthals when archaic and modern populations admixed after 350 kya, suggesting their exclusive link to the modern human niche or that Neanderthal's small population size hindered their spread. Taken together, our results point to a scenario where Modern and Archaic should be regarded as populations of an otherwise common human species, which independently accumulated mutations and cultural innovations.

Introduction:

The acquisition of derived traits has punctuated the long evolutionary path followed by the ancestors of all humans, as witnessed by the fossil record. This constant accumulation of physical, cognitive and cultural innovations is what we collectively refer to when we think of ourselves as "humans". The emerging consensus, corroborated by fossil [1,2,3–5] and molecular [6–8] evidence, sees the emergence of modern humans from an evolutionary branch that split from that of Neanderthal and Denisovans (collectively referred to as archaic humans) around 650 kya[7] (from now on labelled as "Split"). Recent molecular evidence added complexity to this simple split scenario, positing the existence of a deep structure within the human lineage, namely population A and B, with a separation dated to around 1.5 Mya [9]. Population A would be responsible for the entire gene pool of Neanderthals and Denisovans and for 80% of the gene pool of modern humans, while population B would have contributed up to 20% to modern humans, rejoining the main population A about 300 kya. Interestingly, the A/B population structure merger took place before the deepest reported population splits between modern human populations[8], hence featuring among the last major genomic events of our history as a species. As the evolutionary period extending from the separation of modern and archaic human lineages to the earliest splits between modern human populations remains elusive, one may wonder whether it promoted the accumulation of modern human derived elements, or whether such elements were already available before the separation from archaics, rendering, de facto, modern and archaic humans physiologically "human". [10].

In recent years, growing evidence has accumulated in favour of an admixture event between an early modern human lineage and Neanderthals about 350 kya, as witnessed by uniparental (mtDNA and chrY) [11,12,13,14,15] and genomic evidence [12,16–18]. Importantly, this latter introgression occurred as early as 300 ky prior[19] and in the opposite direction with respect to the more widely known human-Neanderthal introgression[20] that followed the Out of Africa expansion of the modern human population. It thus provides an excellent time checkpoint to assess whether the genetic substitutions, accumulated along the modern human lineage after the separation from archaics (Split, **Figure 1A** in dark violet), displayed a high enough adaptive potential to be introgressed and then fixed in the Neanderthal gene pool (**Figure 1A**, in blue). If so, one may postulate that such mutations could yield, at least in part, the answer to what defines us as modern humans. Otherwise, one should conclude that all key genetic substitutions were already present before the Split and were hence shared by modern and archaic humans alike, or that they emerged as a set of modern human-specific substitutions after the Introgression

(either from *de novo* mutation or inherited from population B during the population A/B merger) (**Figure 1A**, in red).
With this work, we set out to exploit the Split and Introgression events to partition human-specific genomic loci [21] and ultimately shed light on the long-lasting question of what makes us human.

Results

Partitioning the genomic landscape of modern and archaic humans

We used the high coverage genomes of Altai Neanderthal and Denisova (Denisova3) as representatives of archaic humans, and of 50 Sub-Saharan individuals from the 1000 Genomes Project as representatives of modern humans. For each individual, we calculated the Time to Most Recent Common Ancestor (TMRCA) with the human reference genome (treated as a random human individual) in 50kbp long windows along the genome (**Figure 1 B, Table S1**). TMRCA estimates were based on pairwise sequence differences and assumed an average genomic mutation rate of 1.25 * 10-8 mut/bp/gen.. We show with coalescent simulations that this simple approach recapitulates the true TMRCA when the top 90% most divergent TMRCA is taken as a summary statistic when 50 modern humans are considered (**Figure 1C**). We excluded from downstream analyses genomic windows with a human-Denisova TMRCA younger than 650 kya, considered enriched in alterations of the local molecular clock (**Figure 1A**). We then focused on genomic windows that showed a TMRCA among modern humans comprised between 650 kya (Split) and 350 kya (Introgression), or more recently than 350 kya (Human650 and Human350 regions, respectively, see Methods and **Figure 1).** This second window was chosen for its potential of having experienced fixation events in modern humans after the Introgression. Of all the genomic windows displaying at least one missense variant with derived frequency >=98% in modern humans and fixed derived in both Altai Neanderthal and Denisova (Figure S1, golden diamond) [22], only a 16 are indeed tagging recent events (Human 650 and Human 350) along the modern human lineage and can be deemed as highly informative in defining what makes us human, additionally showing the high specificity of our approach.

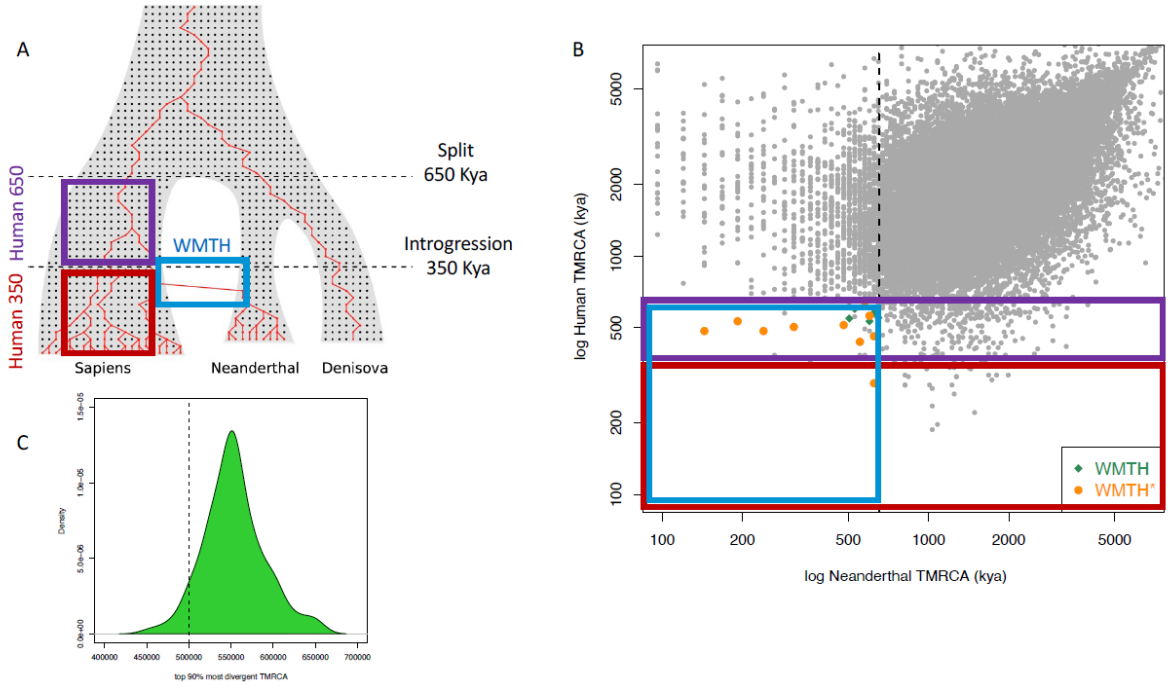

Figure 1 A.**Events Partitioning.** Defining the Split (the separation of modern and archaic lineages, around 650 kya) and the Introgression (the contribution of modern human lineages to the gene pool of Neanderthals, after 350 kya) along the population tree of modern and archaic humans. The gene tree depicted in red exemplifies a Human650 region that entered and was also fixed within the Neanderthal gene pool as a consequence of the Introgression. . B)Scatterplot of the Neanderthal-Human reference (log x-axis) and the Human-Human (log y-axis) TMRCAs on windows displaying a Denisova-Human reference TMRCA >=650 kya. Grey dots represent the bulk of the distribution, which, as expected, is centered around the diagonal for x and y values >=650 kya. Dashed lines report the date of the Split (the separation of modern and archaic humans) along both axes.The top left quadrant is, as expected, enriched by Neanderthal regions introgressed inside the reference sequence, but we assume this signal not to impact our results, since the resulting human-human TMRCA (y-axis) is above the thresholds used for our downstream analyses. Orange dots and green diamonds are the 50 kb regions reported in Table 1 with more (orange) and less (green) stringent criteria (What made them humans, WMTH regions). C) Density plot of the top 90% most divergent TMRCA estimates obtained for every 50-kb window along our 5 Mbp-long simulated genomes. The dotted line indicates the real TMRCA simulated (500,000 years ago).

In addition, we were also interested in how many regions showing a recent human TMRCA (Human650 and Human350) were transferred to the Neanderthal gene pool as a consequence of Introgression, hence displaying versatile and high adaptive potential also in this population of archaic humans. As expected, given the "Introgression" event, we show that Altai Neanderthal displays more regions with a recent coalescence event (<= 650 kya) with the human reference genome than Denisova **(Figure S2,** blue line). This pattern may also be affected by the widespread introgression of Neanderthal alleles into Eurasian genomes [20],

including into a non-negligible portion of the hg19 reference genome used for these analyses (as also visible in the top left quadrant of **Figure 1B and S1**). However, an even more striking difference between the Neanderthal and Denisova signals, which can only be explained as a consequence of the "Introgression", is observed when looking only within Human650 regions (**Figure S2,** green line), which show an excess of reference-Neanderthal recent coalescences compared to reference-Denisova, maxing when the Altai Neanderthal-reference human genome coalescences are around the time of Introgression. Furthermore, within the Human650 regions, the number of regions with a Neanderthal-reference human genome coalescence <= 650 kya (Neanderthal Recent) (n=22) is significantly higher (Fisher exact test, p-value 0.01) than the number of regions (n=7) expected if Human650 and Neanderthal Recent were two independent sets of regions. This result points to the Introgression event having indeed caused a significant number of Human650 regions to have entered the Neanderthal gene pool.

We then tried to single out the Human650 genomic regions that entered the Neanderthal gene pool extracting those with 1) a human reference-Neanderthal coalescence <=650kya, 2) at least one site with derived allele frequency >=98% in modern humans, homozygous derived in Altai Neanderthal and homozygous ancestral in Denisova and 3) no sites with derived allele frequency >=98% in modern humans, homozygous derived in Denisova and homozygous ancestral in Altai Neanderthal. We dubbed these regions "what made them humans" (WMTH), being Human650 regions that contributed to their (Neanderthal's) gene pool. We found ten WMTH regions (**Table 1**, first ten rows, **Figure 1B and S1**, orange dots) that matched all three criteria and an additional seven that matched just the first two criteria (**Table 1**, bottom seven rows marked by an asterisk, **Figure 1B and S1**, green diamonds). Many such regions land on chromosome X, since its smaller population size compared to the autosomes is responsible for a higher coalescence rate. Further validation of the inferred TMRCA of the WMTH regions was performed with Relate (**Supplementary Information, Figure S3**). We also report one region on chromosome X (X:62950000-63000000) that met the WMTH criteria albeit belonging to the Human350 category. We decided to include it in the analysis to avoid spurious threshold effects to be introduced by our decision to partition human regions in Human650 and Human350 mutually exclusive categories.

Table 1. "What made them humans" (WMTH) regions. 17 Human650 regions that contributed to the gene pool of Neanderthals as a consequence of the Introgression event. The last seven regions, highlighted with an

asterisk, display at least one derived site shared between modern humans and Denisova (D-Hder) but not Neanderthal and hence do not meet our full list of inclusion criteria. The abundance of regions landing on chromosome X is explained by the smaller effective population size of its gene pool, which in turn affects the distribution of expected neutral coalescences.

Chr	Start(kb)	End(kb)	NeaTMRCA	DenTMRCA	HumTMRCA	Genes	N-Hder(R,C)	D-Hder(R,C)	Hder(R,C)
5	45600	45650	551834	743851	436800	HCN1	1(0,0)	0(0,0)	4(0,0)
6	27900	27950	239976	3791166	484800	OR2W6P;RPLP2P1;OR2W4P;OR2B6	47(0,0)	0(0,0)	0(0,0)
7	30650	30700	143954	935888	484800	GARS;CRHR2	1(0,0)	0(0,0)	1(0,0)
10	103600	103650	623763	815804	460800	KCNIP2;C10orf76	5(**1**,0)	0(0,0)	0(0,0)
10	103650	103700	599820	791762	561600	C10orf76	8(0,0)	0(0,0)	4(0,0)
12	123550	123600	575896	1127774	643200	RP11-197N18.7;PITPNM2	4(0,0)	0(0,0)	1(0,0)
16	22000	22050	191946	1031670	532800	CTD-2649C14.1;PDZD9;C16orf52	12(0,0)	0(0,0)	0(0,0)
16	22050	22100	311919	1223706	504000	RP11-101E7.2;C16orf52	8(0,0)	0(0,0)	0(0,0)
X	25350	25400	479952	1007798	513600	-	4(0,0)	0(0,0)	7(0,0)
X	62950	63000	623925	671906	292800	ARHGEF9	1(0,0)	0(0,0)	1(0,0)
3*	51650	51700	647857	791842	552000	RAD54L2;TEX264	2(0,0)	**2(0,0)**	2(0,1)
3*	99850	99900	527873	1487613	600000	RP11-15N24.4;CMSS1	13(0,**1**)	**1(0,0)**	0(0,0)
11*	118300	118350	599796	863862	532800	RN7SL86P;ATP5L;RP11-770J1.4;KMT2A	1(0,0)	**1(0,0)**	0(0,0)
X*	81400	81450	623900	2135402	576000	-	26(0,0)	**2(0,0)**	1(0,0)
X*	81500	81550	503859	1511426	547200	-	10(0,0)	**1(0,0)**	7(0,0)
X*	96650	96700	647832	1319525	374400	DIAPH2	10(0,0)	**2(0,0)**	1(0,0)
X*	119650	119700	623888	1439741	600000	CUL4B	14(0,0)	**1(0,0)**	0(0,0)

Abbreviations: *chr: chromosome; NeaTMRCA: time to the most recent common ancestor (TMRCA) between the Altai Neanderthal sequence and the hg19 human reference; DenTMRCA: TMRCA between the Denisova sequence and the hg19 human reference; HumTMRCA: top 90% deepest TMRCA between a panel of 50 African human genomes and the hg19 human reference; N-Hder: sites that are homozygous derived in Altai Neanderthal and have a derived allele frequency of at least 98% in the 1000 Genomes Samples individuals and are homozygous ancestral in Denisova; R,C: of these, how many sites are annotated with Regulatory or Coding consequences (See Table S2 for a full list of these sites); D-Hder: sites that are homozygous derived in Denisova and have a derived allele frequency of at least 98% in the 1000 Genomes Samples individuals and are homozygous ancestral in Altai Neanderthal. All genomic coordinates are in build37 (hg19).*

Functional characterization

Of all the derived alleles shared between Neanderthal and modern humans in WMTH regions, only two (**Table 1**, in bold) were predicted to have regulatory or coding consequences, with one of the two falling in a region not meeting our 3rd inclusion criterion. We asked whether this apparent scarcity of functional mutations is expected when looking at the broader sets of Human650 (**Figure 2**). Overall, WMTH and Human650 regions encompass a similar proportion of functional sites (4.35% and 4.28%, respectively) and the two sets are similar also when looking at the functional sites shared by modern human and Neanderthals, but not Denisovans (FuncHN, Figure 2) (2 regions with at least 1 FuncHN out of 11 WMTH regions (18.2%) versus 60 out of 242 Human650 regions, 24.7%.

Fisher exact test p-value=1). We then characterized the genomic sites that entered the Neanderthal pool during Introgression by computing the ratio of FuncHN against the sum of functional sites where just modern humans (FuncH), modern humans and Neanderthals (FuncHN), or modern humans and Denisovans (FuncHD) shared the derived allele (e.g., all the sites that were derived in modern humans and that could enter the Neanderthal pool during Introgression). The Neanderthal gene pool received significantly fewer modern human-derived functional sites than it could have, given the ones available at the time of Introgression (2 FuncHN out of 177 FuncHN, FuncHD, FuncH or FuncHH in WMTH regions, or 1.13%, compared to 112 FuncH, FuncHD or FuncHN out of 2465 FuncH, FuncHD, FuncHN or FuncHH in Human650, or 4.5%. Fisher exact test p-value=0.03). It follows that, in contrast, WMTH regions showed an excess of derived sites shared by all archaic and modern humans (FuncHH, in gold in Figure 3), hence having occurred along the lineage shared by all archaic and modern humans,here dubbed the *Homo heidelbergensis* (*HH*) lineage. In other words, WMTH regions, a subset of Human650 regions, are not enriched in modern human-derived functional sites. Conversely, and in line with what was observed for human uniparental markers, which were shown to have permeated the gene pool of Neanderthals because of the accumulation of deleterious variants on the latter [15], our results based on autosomal and chromosome X data confirm that Introgression consequences on the Neanderthal gene pool can be best described as a reintroduction of functional variants that were lost in Neanderthal due to the strong genetic drift caused by their reduced effective population size, rather than as an introduction of novel, modern human-specific derived sites.

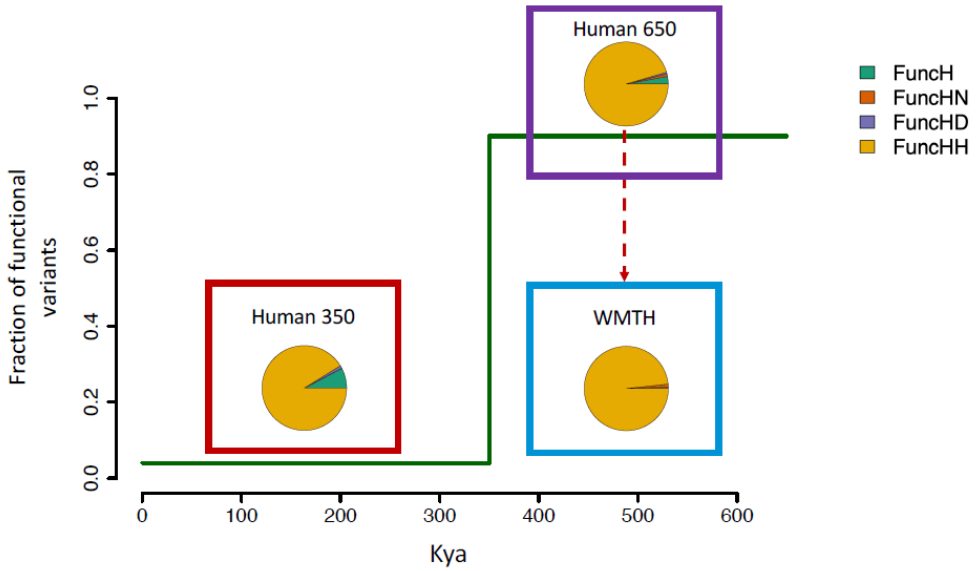

Groups	Sapiens	Neanderthal	Denisova	FuncH	FuncHN	FuncHD	FuncHH	Fraction Total Variants
Human 350	<=350	-	>650	0.08	0.00	0.01	0.91	0.04
WMTH	>350 <=650	<=650	>650	0.01	0.01	0.00	0.98	0.06
Human 650	>350 <=650	-	>650	0.03	0.01	0.01	0.95	0.90

Fig 2. Prevalence of lineage-specific functional variants according to the modern human TMRCA (shown on the x-axis) of the 50 kb window. The green line represents the relative fraction of fixed-derived human functional variants exhibited by the genomic windows showing modern human TMRCA <= 1000 kya. Within each time period, a pie chart represents the breakdown of functional derived sites into FuncH (shared by >98% of modern humans but no archaics; FuncHN, shared by >=98% of modern humans, homozygous derived in Altai Neanderthal and homozygous ancestral in Denisova; FuncHD, shared by >=98% of modern humans, homozygous derived in Denisova and homozygous ancestral in Altai Neanderthal; FuncHH, shared by >=98% of modern humans and homozygous derived in both Denisova and Altai Neanderthal. Most functional variants falling in a Human650 region with a TMRCA in modern humans <= Introgression (Human 350) are shared with all three lineages and only a small portion is unique to modern humans (FuncH). Among the variants with a TMRCA in modern humans between Split and Introgression (Human650), we observe that only a negligible fraction is FuncHN. This fraction is significantly reduced in the WMTH subset (i.e., variants that entered the Neanderthal gene pool during the Introgression).The WMTH subset, on the other hand,shows an enrichment in FuncHH variants.

An interpretation of this emerging picture may imply that the vast majority of modern human-derived variants that experienced a human sweep between Split and Introgression encompassed an adaptive potential that contributed perhaps to the biological characterization of our lineage but that, on the other hand, was either not sufficiently overwhelming to swarm into the Neanderthal gene pool or linked to specific environmental or cultural features of the modern human niche.

To better understand the biological significance of the variants enclosed within Human650 and Human350 regions, we generated protein-protein interaction networks based on genes falling within a Human650 or Human350 region and displaying a coding or regulatory human-derived variant (here defined as being

fixed derived in at least 98% of the 1000 Genomes Project individuals) (**Fig 3**, **Table S2**, **Fig S1**). The resulting list of 56 proteins (**Fig 3)** are, as a whole, significantly enriched in a compelling list of phenotypes (**Fig 3 A**)[23]: the first three (Cognitive impairment, Intellectual disability, Abnormality of higher mental function) are related to higher-level brain function, while the next three (Abnormality of the face, Abnormality of the head, Neurodevelopmental abnormality) are related to developmental anomalies. The 24 proteins associated with one or more of them are highlighted in orange in the network below. Despite these phenotypes appearing to be pivotal aspects to becoming modern humans, only two of these genes (*CMSS1* and *C10orf76*, circled in blue) were passed on to Neanderthals during the Introgression (WMTH regions) and only *CMSS1* is both involved in the above-listed phenotypes and associated with a moderate CADD score (Combined Annotated Dependent Depletion, a measure of the deleteriousness of a mutation)[24] (CADD=3.27, **Table S2**). On the other hand, seven genes involved in the network (*ATRX, SPAG5, ARL13B, TMEM139, ALDOC, STARD7* and *ENOX2*) experienced a human sweep only after Introgression (**Fig S1**, cyan dots), meaning that their functional variants were potentially not available to Neanderthals during the Introgression and for sure did not enter their gene pool. Notably, SPAG5, ATRX and ARL13B interact with and expand the network of proteins for which derived functional variants were already available at the time of the Introgression (**Fig 3 B**). A tempting explanation may involve the role of these latter three genes as the "detonator" to unlock the biological adaptive potential of other genes (namely *MAGT1, RAD54L, SPAG17, DNAH1, SPOP, HDAC*6 and *TCTN1*), that were not sufficient on their own to trigger a sweep in the Neanderthal gene pool after the Introgression. Importantly, *SPAG5* features in several published lists as the gene with the highest number of missense substitutions between modern humans and Neanderthals, and its function has been previously associated with the mitotic spindle [2525,26]. Additional evidence in support of the biological relevance of the modern human-derived allele for the reported SNPs (**Table S2**) is provided by the observation that the vast majority of the functional SNPs falling in the Human650 and Human350 regions display 0% frequency of the ancestral and archaic (Neanderthal or Denisova) allele, even in populations such as Papuan Highlanders [27,28], who experienced introgressions from both populations of archaic humans (**Table S2**).

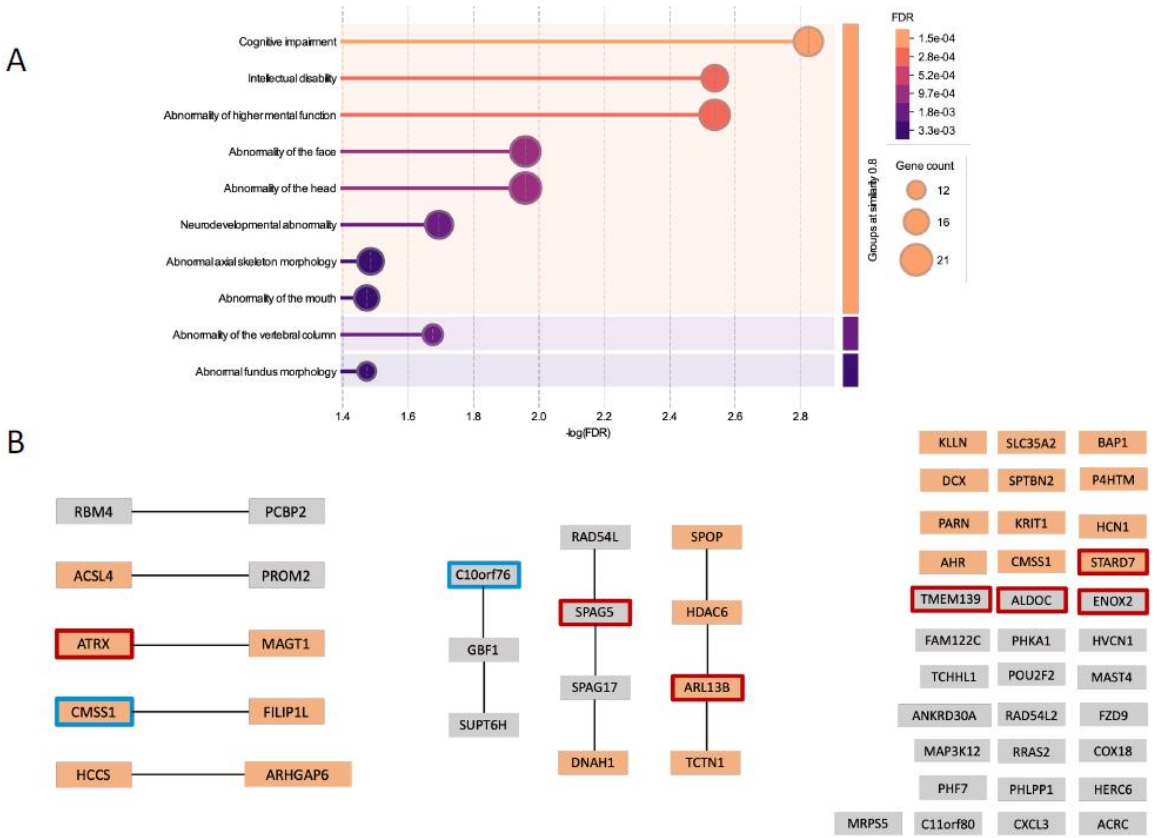

Fig 3. Functional enrichment analyses. A) Functional enrichments of the 56 genes listed in Table S2. Using the STRING database we selected only the phenotypes with a False Discovery Rate (FDR)<=0.05 present in the Monarch phenotypes initiative. The phenotype with the lowest FDR and highest enrichment is cognitive impairment. B) Interaction network obtained from the STRING database using the 56 genes listed in Table S2. Proteins circled in red represent genes with a recent coalescence in humans (Human 350) and proteins circled in blue represent genes defined as WMTH in our manuscript. The 24 orange boxes represent proteins that contribute to at least one of the phenotype enrichments described in panel A.

Newly observed chromosomal rearrangement

Another probable functional consequence of the Introgression is the transfer to the Neanderthal pool, along with the modern human chromosome Y, of the human pseudo-autosomal region 2 (PAR2). Modern human PAR2, like the chromosomal fusion that generated the human chromosome 2, is a genomic rearrangement (X to Y translocation) known to have emerged after the separation of our lineage from the chimpanzee lineage[29]. Together with PAR1, PAR2 enables homologous pairing of the X and Y sex chromosomes during meiosis in human males, but the timing of its translocation event is currently unknown. Firstly, we observed that the male Denisova genome displayed a sequencing depth on regions matching the X chromosome PAR2 higher than the rest of the chromosome (**Supplementary Figure 4**), although not as high (2-fold) as expected. This result may suggest the presence of PAR2 in the Y chromosome of the ancestors of modern and archaic

355 humans unless recurrent acquisition is contemplated[30], but further tests are needed
356 to overcome limitations presented by the extremely low sequencing coverage
357 available for this Denisovan male individual. Similar results obtained for a male
358 Neanderthal genome (**Supplementary Figure 4**) are provided as a control, given
359 that Neanderthal Y chromosome replacement is among the known consequences of
360 the Introgression, and the presence of PAR2 in these archaic populations is
361 therefore amply expected. As PAR1 is present among all modern and archaic
362 human Y chromosomes, given its shared origin with the chimpanzee lineage, we
363 use it as further positive control for our analysis. Once again, we note a
364 comparably higher sequencing depth displayed by all modern and archaic humans
365 at this site (**Supplementary Figure 4)** when compared to the rest of chromosome
366 X, although coverage uncertainties due to the low quality of available ancient DNA
367 are evident.
368 We then set out to provide a molecular dating for the PAR2 translocation and
369 inspected its mutational landscape to characterize the substitutions that occurred
370 since the common ancestor of the PAR2-X sequence that recombined onto
371 chromosome Y. We found 11 SNPs present as heterozygous in male PAR2
372 chromosome X regions and virtually absent in females. These mutations were
373 further attested in Y chromosomes sequenced using long-read platforms[31] their
374 appearance after the translocation event, on the male-specific PAR2 lineage. The
375 identified 11 mutations span a 21,215 bp region at the 5' end of the Y-PAR2 and
376 allowed us to estimate 519 Ky as the time elapsed between i) the separation of the
377 ancestor of all Y-PAR2 sequences from the rest of the X-PAR2 gene pool and ii)
378 the most recent common ancestor of all modern human Y chromosomes, using a Y
379 chromosome mutation rate of 3×10^{-8} mut/bp/gen[32]. To this estimate, we must add
380 338 Ky as the time to the MRCA of all modern human Y chromosomes[33] to
381 provide the full time depth of the translocation event. This region of relatively clear
382 phylogenetic signal is then followed towards the 3' telomeric end of the region by
383 additional mutations with a less polarized frequency difference between males and
384 females, as expected under a scenario of increasing recombination events between
385 the X and Y-PAR2 regions as a function of the genetic distance from the
386 translocation point.
387 Thus, the X->Y PAR2 translocation event must have occurred not earlier than 856
388 kya (95% CI: 633-1253 kya), predating the separation of modern and archaic
389 human lineages. Although the identified polymorphisms likely introduced
390 reference bias, leading to incorrect read mapping and reduced coverage of the PAR
391 regions in the archaic genomes, we could further confirm that the PAR2-Y sites in
392 Spy Neanderthal and Denisova8 shared the expected number of mutations given

their known relationship with the modern human Y chromosome and available coverage (Petr et al. 2020).

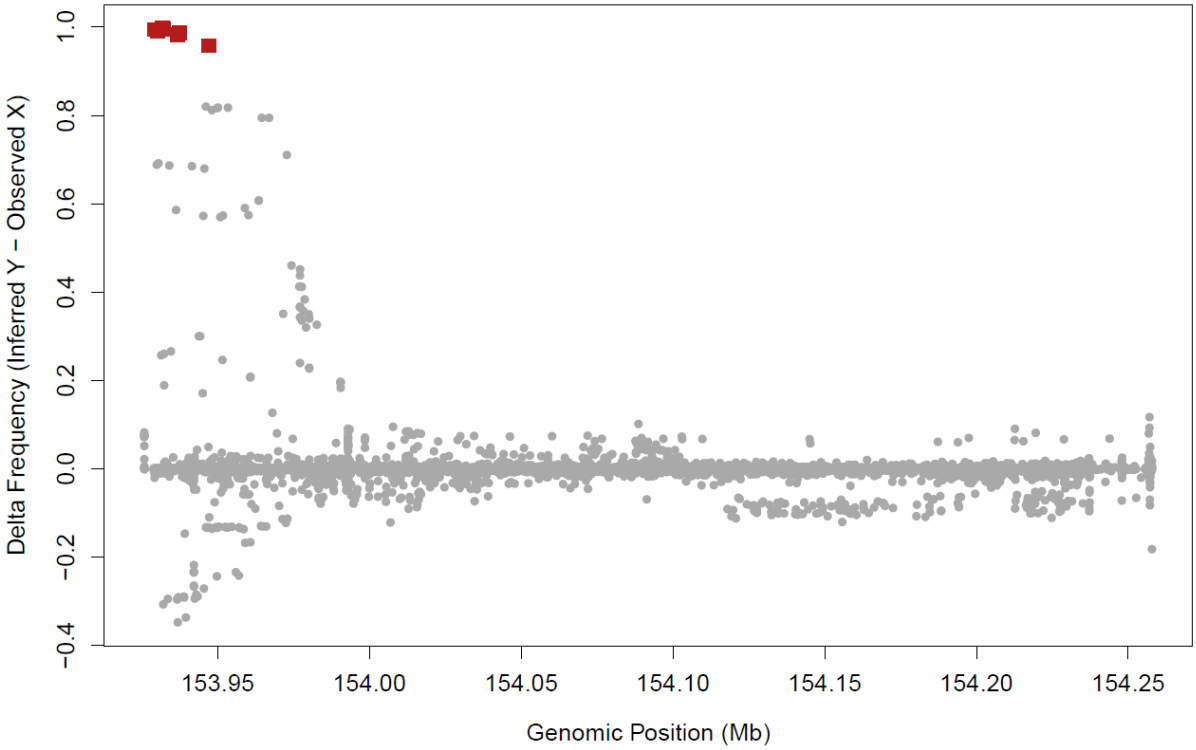

Fig 4. PAR2 Y-specific mutations. Red squares mark the location of the eleven male-specific variants along the ~330 kb long PAR2 sequence when reads from both chromosomes of modern humans are collapsed together. (Red SNP positions: 153929157; 153929840; 153929878; 153930185; 153931728; 153931814; 153932007; 153932008; 153936764; 153937415; 153947049, mapped onto X-PAR2 with T2T-CHM13v2.0 coordinates, with the PAR2 starting point set at 153925834).

Discussion

By integrating the genetic evidence in an evolutionary informed manner, we can organize the derived traits that define us as modern humans in a coherent framework. First, we show that regions that underwent a modern human-specific sweep after the separation from archaic humans (Human650 regions) include at least 24 genes involved in higher-level brain function and morphological development, encompassing coding and regulatory variants. Among the Human650 regions, none were involved in reproduction or fertility pathways, suggesting that gametic isolation was not the primary driver of modern and archaic human divergence.

, we can then investigate whether the derived variants within the Human650 regions enhanced fitness specifically the social and ecological niches of modern humans, or whether they might also have benefited Neanderthals. This question

418 can be addressed by considering the Introgression event (the human-
419 Neanderthal admixture occurred after 350 kya), when these variants had the
420 opportunity to enter the Neanderthal gene pool. We found 17 Human650
421 regions that entered the Neanderthal gene pool (WMTH regions). However,
422 they are not enriched in functional variants and only include 1 of the 24 genes
423 linked with the brain phenotypes mentioned above (circled in blue in Figure
424 3A). Finally, when focusing on highly deleterious SNPs (CADD score>=20)
425 within Human650 regions, we found rs150596428, a missense in SPAG17,
426 rs4413373, a stop gain in HERC6, and rs1782348480, a missense in AHR.
427 None of them fell within the WMTH regions, and only one of them, AHR, was
428 involved in the brain-related phenotype enrichment highlighted in Figure 3.
429 Additionally, the Human650 genomic regions are instead enriched in functional
430 variants that had already emerged before the Split event (modern, Denisovan
431 and neanderthal divergence). These functional alleles were likely lost by genetic
432 drift in the Neanderthal lineage enhanced by their low effective population size.
433 Of note, this affected the OR2B6, GARS, CRHR2, C10orf76, PDZD9 protein-
434 coding genes, among others (see **Supplementary Table S3** for an inclusive
435 list). Our results suggest that the lost functional variants were not an absolute
436 advantage for fitness, since they were not recovered by Neanderthal through
437 introgression with modern humans.
438 We additionally identify modern human-specific sweeps having occurred after
439 the Introgression, which encompass the *SPAG5, ATRX* and *ARL13*B genes.
440 Previous studies suggested secondary gene flows from modern humans into
441 Neanderthals between 100 kya [16] and 200 kya[12]. Regardless of the exact timing
442 of gene flow, we here show that the modern human haplotypes of *SPAG5,*
443 *ATRX* and *ARL13*B did not enter the Neanderthal lineage at a later stage, despite
444 their coalescences in modern humans all precede 200 kya and generally pre-date
445 the deepest separations between present-day modern human populations[8,12].
446
447 Overall, whether or not the human-derived variants in *SPAG5, ATRX* and
448 *ARL13B* ever had the opportunity to express their adaptive potential in
449 Neanderthals, the scenario emerging from this work suggests that modern
450 human-derived functional variants that accumulated over the past 650 kya,
451 particularly those linked to higher brain functions, were most likely tightly
452 linked to the ecological and cultural niche occupied by modern humans in
453 Africa.

454 This notwithstanding, further functional studies are needed to elucidate the
455 putative role of *ATRX, SPAG5* and *ARL13B* as recently acquired keystones of
456 the biological pathways selected by the ecological niche of our human
457 population over the past 650 ky. Indeed, they may have played a role in the fine-
458 tuning of higher-level brain functions, perhaps the most iconic asset of our
459 modern human phenotype.
460 We also caution that our results build on the explicit assumption that modern
461 human defining features must have experienced a sweep after the Split. This
462 strict experimental framework may overlook additional signals that followed a
463 more complex evolutionary history. One example is provided by the *TKL1*
464 locus, which was shown to trigger considerable developmental differences in
465 the brain when the modern or archaic human alleles are deployed [34], but that
466 reached fixation of the derived allele in humans well before the Split (**Table S1**,
467 chrX:153500000-153550000 HumanTMRCA ~1200 kya).
468 As a perspective, given the current limitation in accurately dating derived
469 substitutions fixed across both modern and archaic lineages, the only major
470 events that could be pinpointed as defining the human lineage are the
471 chromosome 2 fusion and the PAR2 translocation. Both events date back over
472 650 kya, predating the modern human, Neanderthal, and Denisovan divergence,
473 and in this sense, they define all of us. Following these events, relaxation of
474 selection due to reduced effective population size in the archaic populations, as
475 well as the accumulation of cultural innovations in both modern and archaics,
476 likely became the main drivers underlying the biological and behavioural
477 differences observed in the archaeological record between what we can consider
478 different populations of a single, cosmopolitan species.
479
480 **Material and Methods**
481
482 **Genomic Data**
483 Publicly available Whole genome sequences (WGS) for modern humans were
484 obtained from https://ftp.1000genomes.ebi.ac.uk/vol1/ftp/release/20130502/ ,
485 WGS for the archaic Neanderthal and Denisova and for the SS6004480 human
486 Chromosome X were obtained from
487 http://cdna.eva.mpg.de/neandertal/altai/Denisovan/ ;
488 http://cdna.eva.mpg.de/neandertal/altai/AltaiNeandertal/VCF/ ;
489 http://cdna.eva.mpg.de/neandertal/Spy94a/;
490 http://cdna.eva.mpg.de/denisova/Den8/;
491 http://cdna.eva.mpg.de/neandertal/altai/ModernHumans/bam/ ;

http://cdna.eva.mpg.de/neandertal/Vindija/VCF/Vindija33.19/.
Genotype calls for the PAR2 were obtained from https://s3-us-west-2.amazonaws.com/human-pangenomics/index.html?prefix=T2T/CHM13/assemblies/variants/1000_Genomes_Project/chm13v2.0/
PAR2 sites were mapped on the T2T-CHM13v2.0 reference. Genomic markers were instead mapped on build hg19 and analyses were run only at sites where the ancestral allele inferred from the 1000 Genomes project was available.

Computing window-based genomic divergences

We computed genetic divergences from the human reference sequence (hg19) by counting the number of differences between the latter and Altai Neanderthal, Denisova or 50 Sub-Saharan African individuals from the 1000 Genomes Project over a sliding window of 50 kb across all the autosomes and chromosome X. We used phased haploid sequences for modern humans and picked a random allele at heterozygous sites in archaic humans. We then converted the resulting divergence estimates ((number of differences/2) / sequence length) in coalescence dates (or time since the most recent common ancestor (TMRCA)) by dividing it by the average human mutation rate (1.25 x 10^{-8} mut/bp/gen)[35] and multiplying it by 30 years, here taken as the human generation time.

$$TMRCA = 30 * \frac{(0.5 * number\ of\ differences)/sequence\ length}{1.25 * 10^{-8}}$$

For each genomic window, we thus obtained a point estimate of the divergence between each archaic human and the reference genome (used as a proxy for a random modern human). We then took the top 90% most divergent estimate based on the 50 African individuals of our dataset as a measure of the within-modern human divergence (humanTMRCA). It is worth noting that we based our humanTMRCA estimates on African genomes to minimize the impact of the Neanderthal introgression that occurred after the expansion of modern humans out of Africa about 60 kya[20,36]. Neanderthal introgressed regions embedded within the reference genome are expected to yield deeper divergences between all tested Africans and the reference genome, but we assumed they would have a marginal impact overall, irrelevant for our experimental design aimed at detecting regions with increased similarity between modern humans and Neanderthals. Eventually, we filtered out from our downstream analyses regions with <50% of accessible sequence based on the 1000 Genomes Project strict accessibility masks (**Table S1**) and <90% availability of archaic and ancestral alleles along all 50 kb sites.

529
530 **Coalescent simulations to validate the obtained TMRCAs**
531 To assess the accuracy of TMRCA estimates based on 50-kb windows, we
532 simulated sequences that had experienced complete selective sweeps 500,000 years
533 ago and inferred their TMRCA based on 50-kb windows.
534 We used msprime[37] to generate 10 diploid chromosomes of length 5 Mbp for 51
535 individuals, assuming a constant recombination rate of $1.25x10^{-8}$ rec/bp/gen, a
536 mutation rate of $1.25x10^{-8}$ mut/bp/gen, a generation time of 30 years, and a
537 constant population size of 15,000 individuals. For each 50-kb window, we
538 simulated a complete selective sweep 500,000 years ago, targeting the middle SNP
539 (using SweepGenicSelection, with a start frequency of 1/2Ne, an end frequency >
540 (2Ne - 1) / (2Ne) (here, 0.999999), a selection coefficient (s) of 1, and a time
541 increment before the sweep (dt) of $1x10^{-6}$). We used one individual as a reference
542 genome to define the genotypes of the 50 remaining individuals as reference or
543 alternative alleles.
544 We then estimated the TMRCA for each 50-kb window along the genome,
545 following the approach described above.
546
547
548
549 **Definition of Human650 and WMTH regions**
550 Based on the data available in **Table S1**, we defined Human650 regions as regions
551 with a) a HumanTMRCA <= 650 kya (i.e., after the separation of our lineage from
552 that of archaic humans, referred to throughout the paper as the "Split") and b) a
553 DenisovaTMRCA >=650 kya (the date range expected from the population tree,
554 Fig. 1A), to exclude genomic regions that experienced apparent relaxation of the
555 molecular clock due to purifying selection.
556 Of these Human650 regions, we further identified What Made Them Human
557 (WMTH) regions as those with i) a NeanderthalTMRCA <=650 kya (not expected
558 on the basis of the population tree, unless human-Neanderthal admixture is
559 involved), ii) at least one fixed derived mutation shared between Altai Neanderthal
560 and modern humans (derived frequency >=0.98 in 1000 Genomes Project
561 individuals) but not Denisovans and iii) no fixed derived mutations shared between
562 Denisovans and modern humans but not Altai Neanderthal.
563
564 **Enrichment analysis**
565 We explored the distribution of archaic/modern and modern/modern TMRCAs
566 computed in **Table S1**, looking for enrichments of Neanderthal/human TMRCA
567 compared to Denisova/human TMRCAs within autosomal loci, hence excluding

568 the X chromosome from this particular analysis. We first examined regions
569 displaying an archaic/human TMRCA falling within a moving cut-off (t) from
570 1000 to 100 kya, with a step of 10 ky and counted the number of 50 kb regions
571 with a NeanderthalTMRCA less than *t* years ago and with DenisovaTMRCA>=650
572 kya, labelled as NRDA (Neanderthal Recent, Denisova Ancient), then we
573 estimated the number of segments with DenisovaTMRCA less than t years ago and
574 with NeanderthalTMRCA >=650 kya, these segments were labelled as DRNA
575 (Denisova Recent - Neanderthal Ancient). We then tested whether the abundance
576 of NRDA and DRNA regions was merely due to Incomplete Lineage Sorting by
577 computing the normalized ratio:

$$Archaic\ recent = {}^{NRDA}/_{(DRNA + NRDA)}$$

578
579 with

$$NRDA = N.segments(NeaTRMCA < T\ \ \&\ \ DenTMRCA \geq 650Kya)$$
$$DRNA = N.segments(DenTRMCA < T\ \ \&\ \ NeaTMRCA \geq 650Kya)$$

580
581 (Blue line in **Supplementary Figure S2)**. A value higher than 0.5 means an excess
582 of NRDA regions compared to DRNA regions.
583 We then computed the same ratio by looking only within Human650 regions and
584 obtained the Archaic Recent within Human650 enrichment curve (Green in
585 **Supplementary Figure 2**).
586
587 **Relate**
588 For each 50kb autosomal WMTH region, we further delved into the analysis of
589 their TMRCA using Relate v1.1.9 [38]. Trees were built for each region of interest
590 using the entire 1000 Genomes dataset (3202 samples) and three archaic genomes.
591 With this, we inferred genomic regions corresponding to each tree (regions with no
592 inferred historical recombination within the sample).
593 We then computed the TMRCA of each tree spanning at least 5kb using the
594 procedure described above (**Supplementary Figure S3**).
595
596 **Variant Annotation and analyses**
597 We used Ensembl VEP (Ensembl GRCh37 release 113)[39] to identify the most
598 severe consequence and the gene associated with each site fixed derived in at least
599 98% of all 1000 Genomes Project individuals and falling in genomic windows with
600 a HumanTMRCA <=1000 kya (i.e., that experienced a human fixation event after
601 Event 1). We subsequently categorized consequences into three main classes:

602 -Coding (missense_variant, splice_acceptor_variant,
603 splice_donor_5th_base_variant, splice_donor_region_variant,
604 splice_donor_variant, splice_polypyrimidine_tract_variant, splice_region_variant,
605 start_lost, stop_gained, stop_lost)
606
607 -Regulatory (3_prime_UTR_variant, 5_prime_UTR_variant,
608 mature_miRNA_variant, regulatory_region_variant, TF_binding_site_variant)
609
610 -Others (downstream_gene_variant, intergenic_variant, intron_variant,
611 non_coding_transcript_exon_variant, synonymous_variant,
612 upstream_gene_variant)
613
614 We referred to Coding and Regulatory consequences together as Functional and
615 distinguished them into four categories: FuncH (>=98% derived allele frequency
616 only in modern humans), FuncHD (>=98% derived allele frequency in modern
617 humans and homozygous derived in Denisova but ancestral in Altai Neanderthal),
618 FuncHN (>=98% derived allele frequency in modern humans and homozygous
619 derived Neanderthals but ancestral in Denisova), and FuncHH (>=98% derived
620 allele frequency in modern humans and homozygous derived in Altai Neanderthal
621 and Denisova).
622
623 We then divided the Functional sites into non-overlapping sets based on the
624 HumanTMRCA and ArchaicTMRCA displayed by the 50 kb windows containing
625 them:
626 Human350: HumanTMRCAs <=350 kya, DenisovaTMRCA >650 kya;
627 Human650 350 kya < HumanTMRCA <= 650 kya and DenisovaTMRCA > 650
628 kya;
629 A final group, called WMTH, was formed by a subset of Human350 regions
630 displaying a NeanderthalTMRCA <= 650 kya.
631
632 To investigate the biological network formed by genes having undergone
633 functional modifications in the past 650 ky of modern human evolution, those
634 affected by at least one FuncH or FuncHN variant of the Human350 and
635 Human650 sets were analyzed using the STRING v12.0 database (STRING
636 database https://string-db.org/). The resulting network of protein-protein
637 interactions was analysed for phenotype enrichment using the STRING enrichment
638 tool against the Monarch Initiative database[40].
639
640 **PAR 2 analyses**

641 We obtained information about sequencing depth along the X chromosomes of a
642 Neanderthal (Spy), a Denisova (Denisova 8), and a modern human male
643 (SS6004480) individual by computing the average depth over non-overlapping 10
644 kb long windows along the whole chromosome X and displayed the distribution of
645 sequencing depth for the PAR1 (X:0-2,394,410), PAR2 (chrX:153,925,834-
646 154,259,566)[41], and remaining portion (chrX:2,394,411-153,925,833) of the X
647 chromosome. To graphically compare the coverage level between the reference
648 modern human, Neanderthal, and Denisova for each of these regions, we scaled it
649 using the *scale* function in R and adding 1 to each value separately.
650 As PAR2 behaves similarly to an autosomal region, it is not possible to distinguish
651 short reads coming from the X-linked from Y-linked PAR2 sequence in a given
652 genome. We therefore retrieved all PAR2-derived reads in modern human male
653 individuals mapping onto the X chromosome, using the most up-to-date set of
654 genotype calls made available by Rhie et al.[41] for the 1000 Genomes Project
655 panel[42]. In practice, we exploited the genotype calls performed by the T2T Y
656 chromosome consortium on all 1000 Genomes Project samples by mapping their
657 reads onto the latest T2T-CHM13v2.0 reference sequence after masking out the
658 chromosome Y-PAR2 region. In this way, we let the X-PAR2 region
659 (chrX:153925834-154259566, almost identical to the Y-PAR2 region
660 chrY:62122809-62460029) attract the relevant reads from either chromosome in
661 both males and females[41].
662 In addition, we estimated allele frequencies for all non-reference PAR2 sites in
663 1000 Genomes Project modern human males and females separately. We used the
664 observed allele frequencies in female and male X chromosomes to infer the allele
665 frequency in male Y chromosomes with the following:
666

667 $$Inferred\ Yfreq = 2 * (Observed\ Male\ X\ freq - Observed\ Female\ X\ freq)$$

668

669 We identified 11 sites that reached an allele frequency in male Y chromosomes
670 close to 1, hence distinguishing Y-PAR2 from X-PAR2 sequences. Other classes
671 of notable mutations, namely the ones showing an X frequency of less than 0.5 in
672 males (inferred to be less than 1 in Y-PAR2) and of approximately 0 in females, as
673 well as the ones showing an X frequency of approximately 0.5 in males (inferred to
674 be approximately 1 in PAR2-Y chromosomes) and of more than 0 in females, were
675 annotated. However, we subsequently discarded them as respectively representing
676 not yet fixed male-specific mutations or mutations present in the X-PAR2 at the
677 time of the translocation, placing them outside of the scope of the present study.
678 The 11 mutations found to be fixed in all surveyed males and virtually absent from

679 females spanned 21,215 bps at the 5' end of the Y-PAR2 sequence and were
680 considered to have occurred since the divergence between X-PAR2 sequences and
681 the most recent common ancestor of all Y-PAR2 sequences - in other words,
682 before the diversification of present-day Y chromosome lineages. We then
683 calculated the time taken for these mutations to accumulate by using the simple
684 formula:
685
686 $$T = g * ((accumulated\ mutations) / length) / mu)$$
687
688 using 30 years as the generation time (g) in humans and ruling out complex back-
689 and-forth scenarios between the X and Y PAR2 pools, given the absence of these
690 mutations within the X-PAR2 gene pool. Using the Y chromosome mutation rate
691 of 3 x 10^{-8} mut/bp/gen[32] yielded a T of 518 ky (95% CI: 295-915 ky) before the
692 MRCA of modern humans. We computed confidence intervals around our estimate
693 by evaluating the probability distribution of observing exactly 11 mutations in
694 21,215 bp over different time intervals and taking the 2.5th and 97.5th quantiles of
695 this distribution. Since the MRCA of modern humans has been attested to date
696 back to338 kya, we eventually obtained a final point estimate of 856 kya as the
697 time of the PAR2 translocation.
698
699
700 **Acknowledgements**
701 The authors would like to thank Prof. Gil Guastoni Rosenthal, Dr. Andra
702 Meneganzin, and Giacomo Moro Mauretto for the fruitful discussions during the
703 drafting of the current manuscript, and Dr. Mathilde André for facilitating access to
704 Papuan allele frequencies. LP was funded by the Italian Ministry of University and
705 Research PRIN N. 2022B27XYM and N. P2022MZCNX.
706
707 **Competing interests:** C. L. is a scientific advisory board member of Nabsys and
708 Genome Insight. The other authors declare that they have no competing interests.
709
710 **Data and materials availability:** All genomic data are publicly available at
711 https://ftp.1000genomes.ebi.ac.uk/vol1/ftp/release/20130502/,
712 http://cdna.eva.mpg.de/neandertal/altai/Denisovan/;
713 http://cdna.eva.mpg.de/neandertal/altai/AltaiNeandertal/VCF/;
714 http://cdna.eva.mpg.de/neandertal/Spy94a/;
715 http://cdna.eva.mpg.de/denisova/Den8/;
716 http://cdna.eva.mpg.de/neandertal/Vindija/VCF/Vindija33.19/, TMRCA
717 computations are available as supplementary data.
718

References

1. Mounier, A. & Mirazón Lahr, M. Deciphering African late middle Pleistocene hominin diversity and the origin of our species. *Nat. Commun.* **10**, 3406 (2019).
2. Hublin, J.-J. *et al.* New fossils from Jebel Irhoud, Morocco and the pan-African origin of Homo sapiens. *Nature* **546**, 289–292 (2017).
3. Vidal, C. M. *et al.* Age of the oldest known Homo sapiens from eastern Africa. *Nature* **601**, 579–583 (2022).
4. White, T. D. *et al.* Pleistocene Homo sapiens from Middle Awash, Ethiopia. *Nature* **423**, 742–747 (2003).
5. Harvati, K. *et al.* Apidima Cave fossils provide earliest evidence of Homo sapiens in Eurasia. *Nature* **571**, (2019).
6. Ragsdale, A. P. *et al.* A weakly structured stem for human origins in Africa. *Nature* **617**, 755–763 (2023).
7. Prufer, K. *et al.* The complete genome sequence of a Neanderthal from the Altai Mountains. *Nature* **505**, 43–49 (2014).
8. Schlebusch, C. M. *et al.* Southern African ancient genomes estimate modern human divergence to 350,000 to 260,000 years ago. *Science* **358**, 652–655 (2017).
9. Cousins, T., Scally, A. & Durbin, R. A structured coalescent model reveals deep ancestral structure shared by all modern humans. *Nat. Genet.* **57**, 856–864 (2025).
10. Meneganzin, A. & Bernardi, M. Were Neanderthals and Homo sapiens ‘good species’? *Quat. Sci. Rev.* **303**, 107975 (2023).
11. Zeberg, H., Jakobsson, M. & Pääbo, S. The genetic changes that shaped Neandertals, Denisovans, and modern humans. *Cell* **187**, 1047–1058 (2024).

744 12. Li, L., Comi, T. J., Bierman, R. F. & Akey, J. M. Recurrent gene flow between
745 Neanderthals and modern humans over the past 200,000 years. *Science* (2024)
746 doi:10.1126/science.adi1768.
747 13. Harris, D. N. *et al.* Diverse African genomes reveal selection on ancient modern
748 human introgressions in Neanderthals. *Curr. Biol.* **33**, 4905–4916.e5 (2023).
749 14. Posth, C. *et al.* Deeply divergent archaic mitochondrial genome provides lower
750 time boundary for African gene flow into Neanderthals. *Nat. Commun.* **8**, 16046
751 (2017).
752 15. Petr, M. *et al.* The evolutionary history of Neanderthal and Denisovan Y
753 chromosomes. *Science* **369**, 1653–1656 (2020).
754 16. Kuhlwilm, M. *et al.* Ancient gene flow from early modern humans into Eastern
755 Neanderthals. *Nature* **530**, 429–433 (2016).
756 17. Hubisz, M. J., Williams, A. L. & Siepel, A. Mapping gene flow between ancient
757 hominins through demography-aware inference of the ancestral recombination
758 graph. *PLoS Genet.* **16**, e1008895 (2020).
759 18. Chen, L., Wolf, A. B., Fu, W., Li, L. & Akey, J. M. Identifying and interpreting
760 apparent Neanderthal ancestry in African individuals. *Cell* **180**, 677–687.e16
761 (2020).
762 19. Reich, D. Hypothesis: A modern human range expansion ~300,000 years ago
763 explains Neandertal origins. *bioRxiv* 2026.03.11.711219 (2026)
764 doi:10.64898/2026.03.11.711219.
765 20. Green, R. E. *et al.* A draft sequence of the Neandertal genome. *Science* **328**,
766 710–722 (2010).
767 21. Weiss, C. V. *et al.* The cis-regulatory effects of modern human-specific variants.
768 *eLife* **10**, (2021).

22. Kuhlwilm, M. & Boeckx, C. A catalog of single nucleotide changes distinguishing modern humans from archaic hominins. *Scientific Reports* **9**, 1–14 (2019).
23. [No title]. https://academic.oup.com/nar/article/52/D1/D938/7449493.
24. Schubach, M., Maass, T., Nazaretyan, L., Röner, S. & Kircher, M. CADD v1.7: using protein language models, regulatory CNNs and other nucleotide-level scores to improve genome-wide variant predictions. *Nucleic Acids Res.* **52**, D1143–D1154 (2024).
25. Peyrégne, S., Kelso, J., Peter, B. M. & Pääbo, S. The evolutionary history of human spindle genes includes back-and-forth gene flow with Neandertals. (2022) doi:10.7554/eLife.75464.
26. Mora-Bermúdez, F. *et al.* Longer metaphase and fewer chromosome segregation errors in modern human than Neanderthal brain development. *Science Advances* (2022) doi:10.1126/sciadv.abn7702.
27. Brucato, N. *et al.* Papua New Guinean Genomes Reveal the Complex Settlement of North Sahul. *Molecular biology and evolution* **38**, (2021).
28. André, M. *et al.* Positive selection in the genomes of two Papua New Guinean populations at distinct altitude levels. *Nat Commun* **15**, 3352 (2024).
29. Otto, S. P. *et al.* About PAR: the distinct evolutionary dynamics of the pseudoautosomal region. *Trends Genet.* **27**, 358–367 (2011).
30. Makova, K. D. *et al.* The complete sequence and comparative analysis of ape sex chromosomes. *Nature* **630**, 401–411 (2024).
31. Hallast, P. *et al.* Assembly of 43 diverse human Y chromosomes reveals extensive complexity and variation. *bioRxiv* 2022.12.01.518658 (2023) doi:10.1101/2022.12.01.518658.
32. Helgason, A. *et al.* The Y-chromosome point mutation rate in humans. *Nat.*

794 *Genet.* **47**, 453–457 (2015).
795 33. Mendez, F. L. *et al.* An African American paternal lineage adds an extremely
796 ancient root to the human Y chromosome phylogenetic tree. *Am. J. Hum. Genet.*
797 **92**, 454–459 (2013).
798 34. Pinson, A. *et al.* Human TKTL1 implies greater neurogenesis in frontal
799 neocortex of modern humans than Neanderthals. *Science* **377**, eabl6422
800 (2022).
801 35. Scally, A. & Durbin, R. Revising the human mutation rate: implications for
802 understanding human evolution. *Nat. Rev. Genet.* **13**, 745–753 (2012).
803 36. Vallini, L. *et al.* The Persian plateau served as hub for Homo sapiens after the
804 main out of Africa dispersal. *Nat. Commun.* **15**, 1882 (2024).
805 37. Baumdicker, F. *et al.* Efficient ancestry and mutation simulation with msprime
806 1.0. *Genetics* **220**, (2022).
807 38. Speidel, L., Forest, M., Shi, S. & Myers, S. R. A method for genome-wide
808 genealogy estimation for thousands of samples. *Nat. Genet.* **51**, 1321–1329
809 (2019).
810 39. McLaren, W. *et al.* The Ensembl Variant Effect Predictor. *Genome Biol.* **17**, 122
811 (2016).
812 40. Mungall, C. J. *et al.* The Monarch Initiative: an integrative data and analytic
813 platform connecting phenotypes to genotypes across species. *Nucleic Acids*
814 *Res* **45**, D712–D722 (2017).
815 41. Rhie, A. *et al.* The complete sequence of a human Y chromosome. *Nature* **621**,
816 344–354 (2023).
817 42. 1000 Genomes Project Consortium, *et al.* A global reference for human genetic
818 variation. *Nature* **526**, 68–74 (2015).

819